

## Angular dependent torque measurements on $\text{CaFe}_{0.88}\text{Co}_{0.12}\text{AsF}$

This content has been downloaded from IOPscience. Please scroll down to see the full text.

2016 J. Phys.: Condens. Matter 28 325701

(<http://iopscience.iop.org/0953-8984/28/32/325701>)

View [the table of contents for this issue](#), or go to the [journal homepage](#) for more

Download details:

IP Address: 106.120.88.146

This content was downloaded on 27/06/2016 at 10:16

Please note that [terms and conditions apply](#).

# Angular dependent torque measurements on $\text{CaFe}_{0.88}\text{Co}_{0.12}\text{AsF}$

HPSTAR  
217-2016

H Xiao<sup>1</sup>, B Gao<sup>1</sup>, Y H Ma<sup>2</sup>, X J Li<sup>2</sup>, G Mu<sup>2</sup> and T Hu<sup>2</sup>

<sup>1</sup> Center for High Pressure Science and Technology Advanced Research, Beijing 100094, People's Republic of China

<sup>2</sup> State Key Laboratory of Functional Materials for Informatics, Shanghai Institute of Microsystem and Information Technology, Chinese Academy of Sciences, Shanghai 200050, People's Republic of China

E-mail: [hong.xiao@hpstar.ac.cn](mailto:hong.xiao@hpstar.ac.cn)

Received 7 April 2016, revised 20 May 2016

Accepted for publication 24 May 2016

Published 24 June 2016



## Abstract

Out-of-plane angular dependent torque measurements were performed on  $\text{CaFe}_{0.88}\text{Co}_{0.12}\text{AsF}$  (Ca1 1 1 1) single crystals. In the normal state, the torque data shows  $\sin 2\theta$  angular dependence and  $H^2$  magnetic field dependence, as a result of paramagnetism. In the mixed state, the torque signal is a combination of the vortex torque and paramagnetic torque, and the former allows the determination of the anisotropy parameter  $\gamma$ . At  $T = 11.5$  K,  $\gamma$  ( $11.5$  K  $\simeq 0.5 T_c$ ) = 19.1, which is similar to the result of  $\text{SmFeAsO}_{0.8}\text{F}_{0.2}$ ,  $\gamma \simeq 23$  at  $T \simeq 0.4T_c$ . So the 1 1 1 1 is more anisotropic compared to 11 and 122 families of iron-based superconductors. This may suggest that the electronic coupling between layers in 1 1 1 1 is less effective than in 11 and 122 families.

Keywords: torque, anisotropy parameter, superconductivity

(Some figures may appear in colour only in the online journal)

## 1. Introduction

In 2006, the first iron-based superconductor (FeSC)  $\text{LaFePO}$  (1 1 1 1) is reported by Hosono's group [1]. In 2008, the breakthrough came with the fluoride doped arsenide  $\text{LaFeAsO}_{1-x}\text{F}_x$  (1 1 1 1) with the superconducting transition temperature up to 26 K [2]. After that many families of FeSCs were discovered but among which  $\text{SmFeAsO}_{1-x}\text{F}_x$  (1 1 1 1) keep the record high of the superconducting transition temperature  $T_c \sim 55$  K [3].  $\text{CaFeAsF}$  is another 1 1 1 1-type of FeSC but is oxygen-free. It has a  $\text{ZrCuSiAs}$ -type tetragonal structure in which LaO layers in  $\text{LaFeAsO}$  are replaced by CaF layers [4]. This parent compound exhibits pressure-induced superconductivity and the maximum  $T_c$  is higher than that in  $\text{LaFeAsO}$ , making it a promising candidate as a parent compound for high  $T_c$  superconductor [5]. Electrons doped into FeAs layers by partial replacement of Fe with Co suppress the antiferromagnetic state and superconductivity arises. In addition, the electronic and magnetic properties of this compound are intermediate between those of  $\text{LaFeAsO}_{1-x}\text{F}_x$  and  $\text{Ba}(\text{Fe}_{1-x}\text{Co}_x)_2\text{As}_2$  [6]. All these features make  $\text{CaFeAsF}$  different from other FeSCs. However, the investigation on this new 1 1 1 1 type of FeSC

are greatly restricted due to the difficulties in obtaining sizable single crystals.

Knowledge of the anisotropy parameter  $\gamma$  is essential to clarify the nature of superconductivity. For the 1 1 1 1 family, limited reports are found on oxypnictides  $\text{LaFeAsO}_{1-x}\text{F}_x$  [7] and  $\text{SmFeAsO}_{0.8}\text{F}_{0.2}$  [7, 8] and there is a discrepancy in the value of  $\gamma$  and also the tendency of temperature dependence. In this paper, we performed detailed torque measurements on  $\text{CaFe}_{0.88}\text{Co}_{0.12}\text{AsF}$  and found that this 1 1 1 1 system is more anisotropic compared to 11 and 122 families of iron-based superconductors where  $\gamma$  stays in the range of 2–3. In addition, we estimated the penetration depth  $\lambda_{ab}$ , which is an important characteristic length scale of a superconductor, which parameterizes the ability of a superconductor to screen an applied field by the diamagnetic response of the superconducting condensate [9].

## 2. Methods

High quality single crystal samples of  $\text{CaFe}_{0.88}\text{Co}_{0.12}\text{AsF}$  were grown using the self-flux method with CaAs as the flux. The details about sample growth and characterization can be found

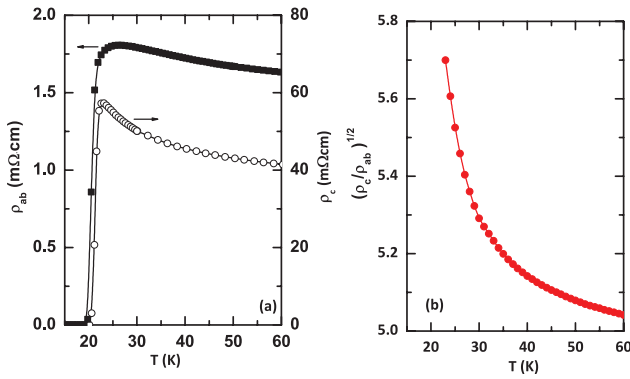


**Figure 1.** (a) Temperature  $T$  dependent in-plane and out-of-plane resistivity data,  $\rho_{ab}$  (left axis),  $\rho_c$  (right axis). (b)  $T$  dependent resistivity anisotropy  $(\rho_c/\rho_{ab})^{1/2}$ .

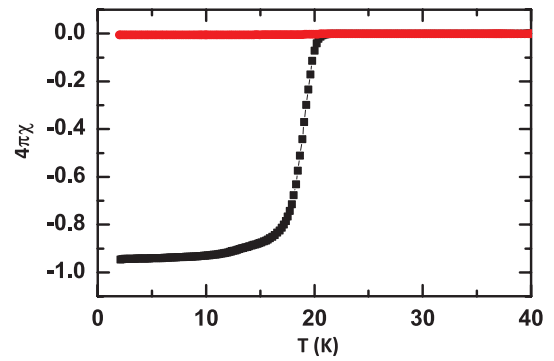


**Figure 2.** Temperature  $T$  dependent normalized magnetization data for  $H = 10$  Oe under both zero-field-cooled (ZFC) and field cooled (FC) conditions.

elsewhere[10]. The actual Co level was determined to be 0.12 through the energy dispersive x-ray (EDX) measurements on the as-grown single crystals. The sample for which the data is shown in this paper has a mass  $m = 0.12 \pm 0.02$  mg. Electrical resistivity measurements were performed in a physical property measurement system (PPMS). Magnetization measurements were performed by using a superconducting quantum interference device (SQUID). Out-of-plane torque measurements were performed using a piezoresistive torque magnetometer in PPMS. The angle  $\theta$  is defined as the angle between the magnetic field and the  $c$  axis of the single crystal.

### 3. Results and discussion

Figure 1(a) shows the temperature  $T$  dependent in-plane and out-of-plane resistivity data  $\rho_{ab}$ ,  $\rho_c$ . An upturn behavior shows up before the transition to the superconducting state for both curves. The onset of the superconducting transition appears at 21.7 K and the zero resistivity is reached at 20.4 K. The anisotropy parameter  $\gamma$  calculated from the normal state resistivity,  $\gamma = \sqrt{\rho_c/\rho_{ab}}$ , is plotted in figure 1(b), which is about 5–6 in the temperature range from 23 to 60 K. This value of  $\gamma$  is similar to the anisotropy of normal state resistivity in  $\text{Ba}_{1-x}\text{K}_x\text{Fe}_2\text{As}_2$ , which is about 3–6 [11]. The magnetization  $M$  curves were measured under field-cooled (FC) and zero-field-cooled (ZFC) conditions with a magnetic field  $H$  of 10 Oe applied along the  $ab$ -plane of the crystal, as shown in figure 2.  $T_c$  determined from magnetization measurements is 20.5 K, which is the same as  $T_{c0}$  of resistivity measurements.

Figure 3(a) shows the typical angular  $\theta$  dependent torque curve  $\tau(\theta)$  of  $\text{CaFe}_{0.88}\text{Co}_{0.12}\text{AsF}$  at temperature above  $T_c$  with an applied magnetic field  $H$  of 9 T. The superconducting transition temperature is  $T_c(9\text{ T}) = 15$  K and the data shown here is for  $T = 30$  K. Note that the torque data is reversible with increasing ( $\tau_{\text{inc}}$ ) and decreasing ( $\tau_{\text{dec}}$ ) angles. Torque  $\tau$  has a  $\sin 2\theta$  angular dependence and can be well fitted by  $\tau_0 \sin 2\theta$ . It is found that  $\tau_0$  has a  $H^2$  magnetic field dependence at  $T = 30$  K, as shown in figure 3(b). These two features,  $\sin 2\theta$  angular dependence and  $H^2$  magnetic field dependence,

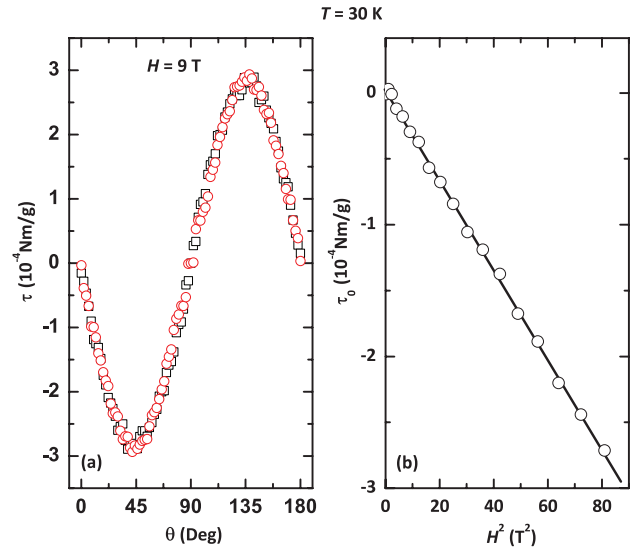


**Figure 3.** (a) Typical angular  $\theta$  dependent torque  $\tau$  at temperature  $T = 30$  K with a magnetic field  $H = 9$  T. (b)  $\tau_0$  versus  $H^2$  at  $T = 30$  K.

are typical behaviors for paramagnetic response  $\tau_p$ , since  $\tau_p = \frac{\chi_c - \chi_a}{2} H^2 \sin 2\theta$ , where  $\chi_c$  and  $\chi_a$  are the susceptibility along the  $c$  and  $a$  axes of the crystal [12, 13]. Since  $\chi_c$  is smaller than  $\chi_a$  in FeSCs, [14] the coefficient of  $\sin 2\theta$  term is negative, which is opposite to the case of the heavy fermion superconductor  $\text{CeCoIn}_5$  [15] and the cuprate superconductor  $\text{Bi}_2\text{Sr}_{2-x}\text{La}_x\text{CuO}_{6+\delta}$ , [16] where  $\chi_c > \chi_a$ .

The anisotropy parameter is an important quantity for characterization and is essential to clarify the nature of superconductivity. We examine the anisotropy of  $\text{CaFe}_{0.88}\text{Co}_{0.12}\text{AsF}$  by studying in detail the torque data for  $T < T_c$ . Figure 4(a) shows the torque data measured at  $T = 16$  K and  $H = 6$  T. A sharp peak around  $90^\circ$  is found and there is large hysteresis between the torque data measured with increasing and decreasing angles ( $\tau_{\text{inc}}$  and  $\tau_{\text{dec}}$ ) as indicated by the arrows. The reversible part of the torque can be obtained by  $\tau_{\text{rev}} = \frac{1}{2}(\tau_{\text{inc}} + \tau_{\text{dec}})$ . Note that only  $\tau_{\text{rev}}$  reflects equilibrium states, which allows the determination of the thermodynamic parameters. Figures 4(b)

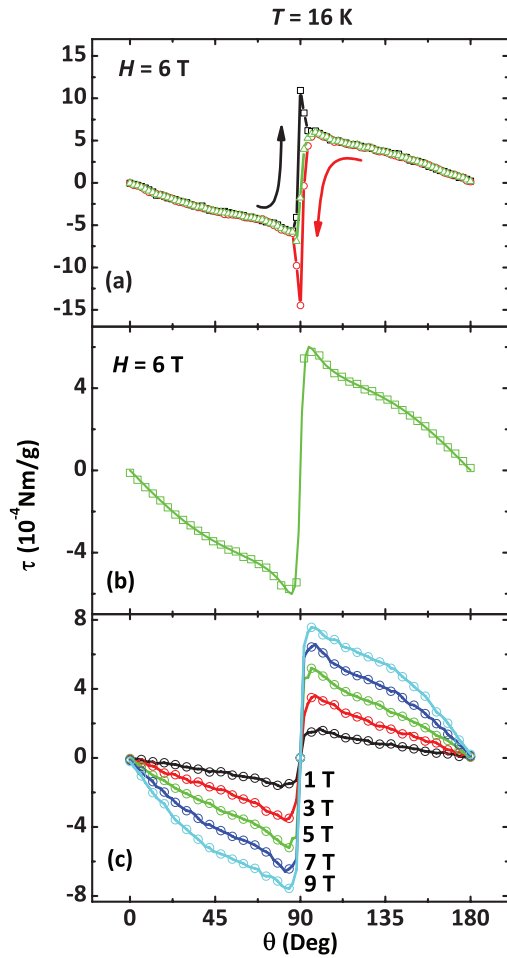


**Figure 4.** Torque data at  $T = 16$  K. (a) Angular  $\theta$  dependent torque data measured at  $H = 6$  T. (b) Reversible part of the torque data  $\tau_{\text{rev}}$  at  $H = 6$  T. (c)  $\tau_{\text{rev}}$  for  $H = 1, 3, 5, 7, 9$  T. In (b), (c) the solid lines are fitting curves by equation (1).

and (c) plots  $\tau_{\text{rev}}$  for the data measured at  $T = 16$  K and with different applied magnetic field. The symbols are data points and the solid lines are fitting curves by the following equation,

$$\tau_{\text{rev}}(\theta) = a \sin 2\theta + \frac{\phi_0 H V}{16\pi\mu_0 \lambda_{ab}^2} \frac{\gamma^2 - 1}{\gamma} \frac{\sin 2\theta}{\epsilon(\theta)} \ln \left\{ \frac{\gamma \eta H_{c2}^{\parallel c}}{H \epsilon(\theta)} \right\}. \quad (1)$$

In the above equation, the first term represents the  $\sin 2\theta$  contribution to the torque signal. The second term describes the vortex torque according to Kogan's model [17] which is derived in the frame of the anisotropic Ginzburg–Landau regime, where  $\mu_0$  is the vacuum permeability,  $\lambda_{ab}$  is the penetration depth in the  $ab$ -plane,  $\gamma = \sqrt{m_c/m_a}$  is the anisotropy parameter ( $m_c$  and  $m_a$  is the effective mass along the  $c$  and  $a$  axes),  $\epsilon(\theta) = (\sin^2 \theta + \gamma^2 \cos^2 \theta)^{1/2}$ ,  $\eta$  is a numerical parameter of the order of unity, and  $H_{c2}^{\parallel c}$  is the upper critical field parallel to the  $c$ -axis.

We use  $\gamma$ ,  $a$  and  $\lambda_{ab}$  as fitting parameters to fit the torque data and figures 4(b) and (c) shows the fitting results. Note that the contribution from the  $\sin 2\theta$  term becomes more

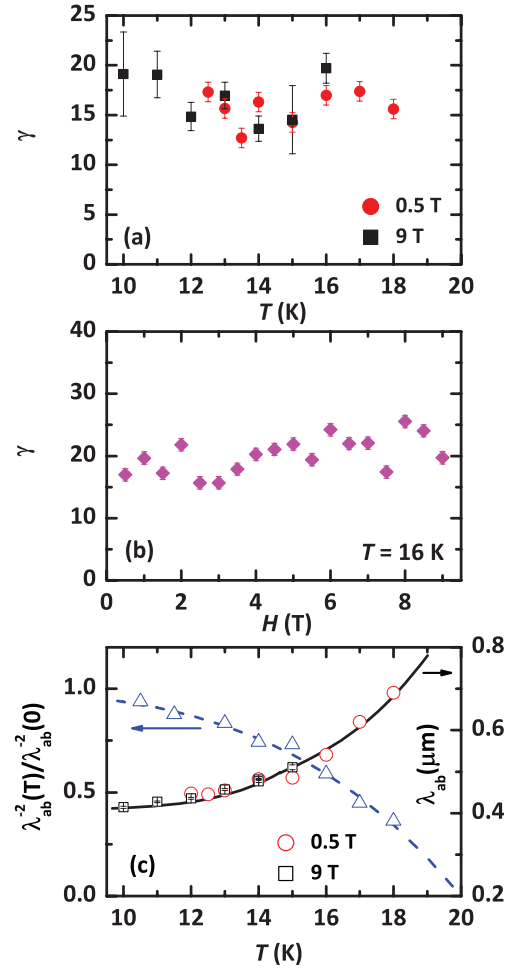


**Figure 5.** (a) Temperature  $T$  dependence of anisotropy parameter  $\gamma$ . (b) The magnetic field  $H$  dependence of  $\gamma$ . (c) Right axis: temperature dependence of penetration depth  $\lambda_{ab}$ . Left axis: temperature dependence of the normalized superfluid density  $\lambda_{ab}^{-2}(T)/\lambda_{ab}^{-2}(0)$ . The dashed line is a fitting curve by equation (2).

evident as the magnetic field increases. We summarize the temperature and magnetic field dependence of the anisotropy parameter  $\gamma$  in figures 5(a) and (b). It is found that  $\gamma$  shows weak temperature and magnetic field dependence. At  $T = 11.5$  K,  $\gamma(11.5 \text{ K} \simeq 0.5T_c) = 19.1$ , which is similar to the result of  $\text{SmFeAsO}_{0.8}\text{F}_{0.2}$ ,  $\gamma \simeq 23$  at  $T \simeq 0.4T_c$  [8]. So, the 1 1 1 1 is more anisotropic in the superconducting state compared to 11 and 122 families of FeSCs, where  $\gamma$  stays in the range of 2–3 as evidenced by  $\mu\text{SR}$  measurements, [18] despite the fact that the normal state anisotropy parameter is about the same in the 1 1 1 1 and 122 compounds ( $\gamma$  is 5–6 for the former and 3–6 for the latter). This might suggest that in the superconducting state, the electronic coupling between layers in 1 1 1 1 is less effective than in the 11 and 122 families.

Figure 5(c) (right axis) shows temperature dependence of the penetration depth  $\lambda_{ab}$ , which is obtained from fits of equation (1) to the torque data. The left axis shows the temperature dependence of normalized superfluid density  $\lambda_{ab}^{-2}(T)/\lambda_{ab}^{-2}(0)$ . It is found that  $\lambda_{ab}^{-2}(T)/\lambda_{ab}^{-2}(0)$  decreases with

increasing temperature and vanishes when approaching  $T_c$ . We use the empirical equation,

$$\lambda_{ab}^{-2}(T)/\lambda_{ab}^{-2}(0) = 1 - (T/T_c)^n \quad (2)$$

with  $n = 4$  to fit our data (see the dashed line) and obtain  $\lambda(0) = 400$  nm. Lower critical field measurements on  $\text{PrFeAsO}_{1-y}$  give  $\lambda(0) = 280$  nm [19]. From  $\mu\text{SR}$  measurements,  $\lambda(0) = 189$  and 195 nm for  $\text{SmFeAsO}_{0.85}$  and  $\text{NdFeAsO}_{0.85}$  [20];  $\lambda(0) = 254$  and 364 nm for  $\text{LaFeAsO}_{1-x}\text{F}_x$   $x = 0.1$  and 0.075 [21]. Our result of  $\lambda_{ab}$  here is comparable with that of other 1 1 1 1 families.

#### 4. Conclusions

In summary, we performed detailed angular dependent torque measurements on  $\text{CaFe}_{0.88}\text{Co}_{0.12}\text{AsF}$ . A large paramagnetic effect is observed in the normal state. After subtracting this paramagnetic contribution to the mixed state, we obtain the anisotropy parameter from the mixed state torque data and summarized its temperature and magnetic field dependence. The value of  $\gamma$  is comparable with other 1 1 1 1 families of FeSCs, but much larger than 11 and 122 families of FeSCs. The zero temperature penetration depth of  $\text{CaFe}_{0.88}\text{Co}_{0.12}\text{AsF}$  is also estimated, which is reasonable when compared to the value reported for other 1 1 1 1 FeSCs.

#### Acknowledgments

The authors acknowledge the support of NSFC, Grant No. U1530402, 11574338 and 11204338; MOST of China, Project No. 2015CB921303 the ‘Strategic Priority Research Program (B)’ of the Chinese Academy of Sciences (no. XDB04040300, XDB 04040200 and XDB 04030000) and the Youth Innovation Promotion Association of the Chinese Academy of Sciences (no. 2015187).

#### References

- [1] Kamihara Y, Hiramatsu H, Hirano M, Kawamura R, Yanagi H, Kamiya T and Hosono H 2006 *J. Am. Chem. Soc.* **128** 10012
- [2] Yoichi Kamihara A T W, Hirano M and Hosono H 2008 *J. Am. Chem. Soc.* **130** 3296
- [3] Ren Z-A *et al* 2008 *Chin. Phys. Lett.* **25** 2215
- [4] Matsuishi S, Inoue Y, Nomura T, Yanagi H, Hirano M and Hosono H 2008 *J. Am. Chem. Soc.* **130** 14428
- [5] Okada H, Takahashi H, Matsuishi S, Hirano M, Hosono H, Matsubayashi K, Uwatoko Y and Takahashi H 2010 *Phys. Rev. B* **81** 054507
- [6] Nakano T, Tsutsumi S, Fujiwara N, Matsuishi S and Hosono H 2011 *Phys. Rev. B* **83** 180508
- [7] Li G, Grissonnanche G, Gurevich A, Zhigadlo N D, Katrych S, Bukowski Z, Karpinski J and Balicas L 2011 *Phys. Rev. B* **83** 214505
- [8] Weyeneth S, Puzniak R, Mosele U, Zhigadlo N, Katrych S, Bukowski Z, Karpinski J, Kohout S, Roos J and Keller H 2009 *J. Supercond. Novel Magn.* **22** 325
- [9] Hashimoto K *et al* 2013 *Proc. Natl Acad. Sci.* **110** 3293
- [10] Ma Y, Hu K, Ji Q, Gao B, Zhang H, Mu G, Huang F and Xie X 2016 (arXiv:1605.04642v1)
- [11] Zverev V N, Korobenko A V, Sun G L, Sun D L, Lin C T and Boris A V 2011 *Japan. J. Appl. Phys.* **50** 05FD02
- [12] Kasahara S *et al* 2012 *Nature* **486** 382
- [13] Okazaki R, Shibauchi T, Shi H J, Haga Y, Matsuda T D, Yamamoto E, Onuki Y, Ikeda H and Matsuda Y 2011 *Science* **331** 439
- [14] Sefat A S, Jin R, McGuire M A, Sales B C, Singh D J and Mandrus D 2008 *Phys. Rev. Lett.* **101** 117004
- [15] Xiao H, Hu T, Almasan C C, Sayles T A and Maple M B 2006 *Phys. Rev. B* **73** 184511
- [16] Xiao H, Hu T, Zhang W, Dai Y M, Luo H Q, Wen H H, Almasan C C and Qiu X G 2014 *Phys. Rev. B* **90** 214511
- [17] Kogan V G 1988 *Phys. Rev. B* **38** 7049
- [18] Khasanov R and Guguchia Z 2015 *Supercond. Sci. Technol.* **28** 034003
- [19] Okazaki R *et al* 2009 *Phys. Rev. B* **79** 064520
- [20] Khasanov R, Luetkens H, Amato A, Klauss H-H, Ren Z-A, Yang J, Lu W and Zhao Z-X 2008 *Phys. Rev. B* **78** 092506
- [21] Luetkens H *et al* 2008 *Phys. Rev. Lett.* **101** 097009